ACS APPLIED BIO MATERIALS
Cite This: ACS Appl. Bio Mater. 2018, 1, 33−41
Article
www.acsabm.org

Fouling-Resistant Hydrogels Prepared by the Swelling-Assisted Infusion and Polymerization of Dopamine

Kristopher W. Kolewe,[†] Kerianne M. Dobosz,[†] Todd Emrick,[‡] Stephen S. Nonnenmann,[§] and Jessica D. Schiffman*[,†]

[†]Department of Chemical Engineering, University of Massachusetts Amherst, Amherst, Massachusetts 01003-9303, United States
[‡]Department of Polymer Science & Engineering, Conte Center for Polymer Research, 120 Governors Drive, University of Massachusetts Amherst, Amherst, Massachusetts 01003-9303, United States
[§]Department of Mechanical and Industrial Engineering, University of Massachusetts Amherst, Amherst, Massachusetts 01003-9303, United States

Supporting Information

ABSTRACT: Biofilm-associated infections stemming from medical devices are increasingly challenging to treat due to the spread of antibiotic resistance. In this study, we present a simple strategy that significantly enhances the antifouling performance of covalently cross-linked poly(ethylene glycol) (PEG) and physically cross-linked agar hydrogels by incorporation of the fouling-resistant polymer zwitterion, poly(2-methacryloyloxyethyl phosphorylcholine) (pMPC). Dopamine polymerization was initiated during swelling of the hydrogels, which provided dopamine and pMPC, an osmotic driving force into the hydrogel interior. Both PEG and agar hydrogels were synthesized over a broad range of storage moduli (1.7−1300 kPa), which remained statistically equivalent after being functionalized with pMPC and polydopamine (PDA). When challenged with fibrinogen, a model blood-clotting protein, the pMPC/PDA-functionalized PEG and agar hydrogels displayed a >90% reduction in protein adsorption compared to hydrogel controls. Further, greater than an order-of-magnitude reduction in *Escherichia coli* and *Staphylococcus aureus* adherence was observed. This study demonstrates a versatile material platform to enhance the fouling resistance of hydrogels through a pMPC/PDA incorporation strategy that is independent of the chemical composition and network structure of the original hydrogel.

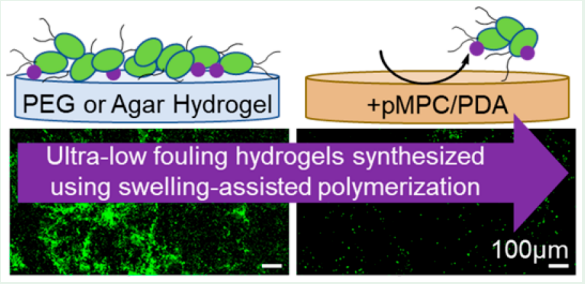

KEYWORDS: *antifouling, dopamine, hydrogel, microorganism, poly(ethylene glycol), zwitterion*

INTRODUCTION

Indwelling medical devices are indispensable tools in modern healthcare. However, the insertion of any foreign object into the human body carries an inherent risk of infection.[1−3] Over one-quarter of all healthcare-associated infections in the United States are attributed to central line-associated bloodstream infections and catheter-associated urinary tract infections.[4−6] Hydrogel coatings are typically applied to catheters to improve patient comfort while also mitigating nonspecific protein adsorption and bacterial adhesion.[7−9] The gold standard hydrophilic polymer used for antifouling coatings is poly(ethylene glycol) (PEG),[10] since it hydrogen bonds with water to create a hydration layer that prevents nonspecific protein adsorption.[11,12] Surface hydration limits bacterial adherence to PEG coatings. Although surface chemistry is critical to controlling bacterial adhesion, the morphological and mechanical properties of a material will also influence bacterial surface interactions. Previously, we and others demonstrated that independent of hydrogel chemistry softer hydrogels experience a slower rate bacterial colonization by *Escherichia coli* (*E. coli*) and *Staphylococcus aureus* (*S. aureus*).[13−16] This work determined that the fouling resistance of PEG hydrogels can be improved further by harnessing fundamental structure−property relationships. However, given sufficient time, bacteria will colonize on low-fouling hydrophilic coatings, including PEG. To combat these microorganisms, commercial antibiotic treatments have been overused, which has accelerated the evolution of resistant genes in bacterial species.[17,18] Thus, new materials that delay the initial attachment of proteins and microorganisms, while avoiding the spread of resistant genes, are in demand.

Polymer zwitterions have emerged as a promising class of antifouling polymers due to their enhanced stability and excellent fouling resistance.[19,20] Carrying both positive and negative charges on each monomer subunit, polymer zwitterions induce a tight and stable surface hydration layer of "surface-bound" water that effectively resists protein adsorption.[21,22] Although previously synthesized zwitterion-

Received: April 17, 2018
Accepted: June 8, 2018
Published: June 8, 2018

DOI: 10.1021/acsabm.8b00001
ACS Appl. Bio Mater. 2018, 1, 33−41

containing hydrogels effectively decreased biofouling, many exhibited poor mechanical strength.[23−26] Thus, clay-nanocomposites,[27] double-networks,[28] functional cross-linkers,[29] and pH-responsive monomers have been incorporated into zwitterion-containing hydrogels, which enhanced their mechanical strength by 2−3 times.[30] However, these strategies require designer synthesis, limiting their compatibility with existing hydrogels. The ability to integrate zwitterionic functionality into any hydrogel, irrespective of its chemistry or cross-linking structure, would extend the benefits of polymer zwitterions across the entire class of hydrogels.

Polydopamine offers an attractive universal approach to surface functionalization. Lee et al. reported that under alkaline conditions, dopamine undergoes oxidative polymerization into an ultrathin surface-adherent polydopamine film on virtually any abiotic or biotic surface.[31,32] With the utilization of the functionality of polydopamine, the facile immobilization of molecules containing carboxyl, amine, thiol, quaternary ammonium, and/or catechol groups has been immobilized into functional coatings.[33−37] Further studies have demonstrated the superior antifouling performance of similar coatings applied to a diverse array of solid materials including glass, silicon, steel, and polymer nanofibers.[33,35,38] Although catechol cross-linkers, including dopamine, have been examined in numerous hydrogel formulations,[39−41] the versatility of polydopamine-containing coatings presents a potentially universal hydrogel modification strategy.

In this work, we demonstrate a simple and robust approach to enhance the antifouling performance of PEG and agar hydrogels that uses the polymerization of dopamine to immobilize the fouling-resistant polymer zwitterion, poly(2-methacryloyloxyethyl phosphorylcholine) (pMPC). By initiating dopamine polymerization while swelling the hydrogels, dopamine and pMPC are osmotically driven into the hydrogel interior and become immobilized. The incorporation of pMPC statistically improves the fouling resistance of PEG and transforms agar from a high-fouling to a fouling-resistant hydrogel. This simple technique represents a versatile approach to improve the antifouling performance of hydrogels, irrespective of their chemistry, network structure, and mechanical properties.

MATERIALS AND METHODS

Materials and Chemicals. Poly(ethylene glycol) dimethacrylate, (PEG, M_N = 750 Da), dopamine hydrochloride (dopamine), 3-(trimethoxysilyl)propyl methacrylate, ampicillin (BioReagent grade), chloramphenicol (BioReagent grade), M9 minimal salts (M9 media), D-(+)-glucose, calcium chloride (anhydrous), phosphate buffered saline (PBS, 10× sterile biograde), tryptic soy broth (TSB), Luria−Bertani broth (LB), fibrinogen, and Bradford reagent were purchased from Sigma-Aldrich (St. Louis, MO). Irgacure 2959 was obtained from BASF (Ludwigshafen, Germany). Anhydrous magnesium sulfate and molecular grade agar were obtained from Fisher Scientific (Fair Lawn, NJ). Deionized (DI) water was obtained from a Barnstead Nanopure Infinity water purification system (Thermo Fisher Scientific, Waltham, MA).

Fabrication of pMPC/PDA-Modified PEG and Agar Hydrogels. PEG hydrogels were prepared using previously established protocols.[16] Briefly, 8.3, 28, and 55 wt % PEG dimethacrylate in 10 mM PBS (pH = 7.4) was filtered through a sterile 0.2 μm membrane and then degassed using nitrogen. For UV-curing, Irgacure 2959 (0.8 wt %) was added to the polymer precursor solution with induction under a longwave UV light (365 nm) for 10 min. The PEG solution (75 μL) was sandwiched between two 22 mm UV-sterilized coverslips (Fisher Scientific) functionalized with 3-(trimethoxysilyl)propyl methacrylate.[42] Fabricating the hydrogel between coverslips enabled all hydrogels to have a uniform thickness of ∼150 μm and limited their oxygen exposure. Agar hydrogels were prepared by dissolving 1.0, 3.0, and 9.0 wt % agar in sterile DI water for 30 min before uniformly heating the solution in a liquid autoclave at 250 °C for 30 min. The hot solution was cast into glass Petri dishes (Pyrex, Tewksbury, MA) and allowed to gel at a uniform height of 2 mm. After the agar cooled, a flame-sterilized punch (Spearhead 130 Power Punch MAXiset, Cincinnati, Ohio) was used to create circular 25.4 mm diameter agar hydrogels.

pMPC was synthesized as previously described.[34,43] The unmodified PEG and agar hydrogels were placed into 6-well polystyrene plates (Fisher Scientific) and immersed in 5 mL of Tris buffer (10 mM, pH 8.5) containing only dopamine (2 mg/mL) or solutions containing both dopamine (2 mg/mL) and pMPC (2 mg/mL) for 6 h. Under these basic conditions, dopamine undergoes oxidative self-polymerization to form polydopamine (PDA) when alone in solution or forms composites through noncovalent interaction when in the presence of pMPC.[34] All hydrogels were removed from the reaction solution and washed 3 times with DI water before being placed in a new 6-well plate at 23 °C with DI water until further testing. In the Results section, PEG and agar hydrogels are referred to as unmodified, PDA (if functionalized only with dopamine), or pMPC/PDA (if functionalized with dopamine and pMPC).

Characterization of pMPC/PDA-Modified PEG and Agar Hydrogels. The chemical compositions of unmodified, PDA, and pMPC/PDA PEG and agar hydrogels were determined using a PerkinElmer Spectrum 100 Fourier transform infrared spectrometer (FTIR, Waltham, MA). All spectra were recorded from 4000 to 500 cm^{-1} by accumulation of 32 scans and with a resolution of 4 cm^{-1}. Scans were performed in duplicate on three replicates for each hydrogel. To monitor if the fabrication method had diffusion limitations, hydrogels were fabricated in cylindrical molds (2 mm thick and 22 mm in diameter) from 8.3 and 55 wt % PEG, as well as from 1.0 and 9.0 wt % agar. Following polymerization, hydrogels were swollen in 5 mL of Tris buffer containing 2 mg/mL of dopamine. After 1, 6, and 24 h, the hydrogels were removed from solution and gently rinsed with DI water. The hydrogel's top surface, bottom surface, and cross section were photographed (Nikon D5200 camera with an AF-S NIKKOR 18−35 mm 1:3.5−5.6G lens) and the red-green-blue (RGB) color values were quantified using Adobe Photoshop CC 2017.

Equilibrium swelling experiments were performed to determine the volumetric swelling ratio, Q, of unmodified, PDA, and pMPC/PDA PEG hydrogels. The unmodified, free-standing PEG hydrogels were swollen in PBS for 24 h at 23 °C until equilibrium swelling was achieved and were then weighed to obtain their equilibrium swelling mass, M_S. These hydrogels were lyophilized (Labconco, FreeZone Plus 2.5 Liter Cascade Console Freeze-Dry System, Kansas City, MO) for 72 h and then weighed to determine their dry mass, M_D. Q was calculated by dividing M_S by M_D. To quantify Q for PDA and pMPC/PDA hydrogels, the unmodified PEG hydrogels were weighed directly following polymerization to obtain the weight of the unmodified PEG hydrogel. Following the 6 h functionalization, hydrogels were washed 3 times with DI water and immersed in PBS for 48 h before being weighed to determine M_S. Hydrogels were then lyophilized and weighed to determine M_D. Four replicates were tested for each hydrogel.

Small amplitude oscillatory shear (SAOS) measurements were acquired on the PEG and agar hydrogels using a plate−plate geometry with a diameter of 20 mm and a gap of 1 mm (Kinexus Pro rheometer, Malvern Instruments, U.K.). Prepared hydrogels (circular 25 mm diameter × 1 mm height) were loaded into the rheometer and trimmed to size using a razor blade. A strain amplitude sweep was performed to ensure that experiments were conducted within the linear viscoelastic region at a strain of 0.1%. Oscillation frequency sweeps were conducted over an angular frequency domain 1.0 and 100 rad/s at 23 °C.

DOI: 10.1021/acsabm.8b00001
ACS Appl. Bio Mater. 2018, 1, 33−41

The size of PDA aggregates on the surface of hydrogels was measured using an atomic force microscope (Cypher ES AFM, Asylum Research/Oxford Instruments, Santa Barbara CA) equipped with a PerFusion attachment for complete sample immersion. Topographic imaging was performed in DI water at room temperature (~23 °C) using TR800PSA (k = 183.54 pN/nm) cantilevers (Olympus, Tokyo, Japan). Hydrogels were prepared on 15 mm glass coverslips and remained hydrated throughout the entire AFM preparation and testing process. Micrographs of hydrogels and hydrogel cross sections were acquired using a Magellan 400 XHR scanning electron microscope (FEI, Hillsboro, OR). Cross sections were obtained by flash-freezing the hydrogels using liquid nitrogen and then cracking the sample. Hydrogels were sputter-coated for 60 s with platinum before SEM imaging (Cressington 208 HR, Cressington Scientific Instruments, Watford, U.K.).

Evaluation of Protein Adsorption and Bacterial Resistance of pMPC/PDA-Modified PEG and Agar Hydrogels. Protein adsorption was quantified using a fluorescent protein assay. Circular 15 mm diameter PEG and 12.7 mm diameter agar hydrogels were placed at the bottom of 24-well plates, to which 55 μL of fluorescently tagged fibrinogen (~2 tags per protein)[44,45] in PBS (655 μg/mL) was added and agitated at 100 rpm for 48 h at 23 °C. The hydrogels were surface rinsed 3 times with PBS; then the adsorption of fibrinogen was assessed using a Zeiss Microscope Axio Imager A2M (20× magnification, Thornwood, NY). Experiments were conducted in triplicate.

Bacterial adhesion was evaluated using the model Gram-negative strain *Escherichia coli* K12 MG1655 (*E. coli*, DSMZ, Leibniz-Institut, Germany) containing a GFP plasmid and the model Gram-positive strain *Staphylococcus aureus* SH1000 (*S. aureus*) containing the high-efficiency pCM29 sGFP plasmid.[46] Circular 22 mm diameter control and pMPC/PDA PEG and agar hydrogels were placed at the base of 6-well polystyrene plates, to which 5 mL of M9 media with 100 μg/mL of ampicillin, or 10 μg/mL of chloramphenicol, were added for *E. coli* or *S. aureus*, respectively. The growth media in each well was inoculated with an overnight culture with a working concentration of 1.00×10^8 cells/mL (*E. coli* or *S. aureus*), which were washed and resuspended in M9 media[47] and then placed in an incubator at 37 °C for 24 h. Hydrogels with attached bacteria were removed from the 6-well polystyrene plates and rinsed lightly using PBS to remove loosely adhered bacteria. *E. coli* and *S. aureus* attachment was evaluated using a modified adhesion assay that monitored bacteria colony coverage (Zeiss Axio Imager, 20× magnification). The particle analysis function in ImageJ 1.48 software (National Institutes of Health, Bethesda, MD) was used to calculate the bacteria colony area coverage over the acquired 58 716 μm^2 area.[48,49] Significant differences between samples were determined using an unpaired student t-test.

RESULTS AND DISCUSSION

Characteristics of pMPC/PDA-Modified PEG and Agar Hydrogels. Chemically and physically cross-linked hydrogels were successfully synthesized from PEG dimethacrylate (8.3, 28, and 55 wt %) and from agar (1.0, 3.0, and 9.0 wt %), respectively. Chemical functionalization of these hydrogels was achieved through a process we coined "swelling-assisted polymerization". By immersing the hydrogels in Tris buffer, containing 2 mg/mL of dopamine and poly(2-methacryloyloxyethyl phosphorylcholine) (pMPC), the resulting concentration gradient induced an osmotic driving force into the hydrogel that facilitated pMPC/PDA formation throughout the polymer network.

The successful polymerization of dopamine to polydopamine (PDA) throughout the PEG and agar hydrogels was apparent due to their brown color, which is characteristic of the melanin-like structure of PDA, Figure 1. Fourier transform infrared spectroscopy (FTIR), Figure S1, acquired on the pMPC/PDA-functionalized PEG and agar hydrogels did not show pronounced peaks after functionalization, likely a result of the low concentration of the pMPC/PDA.[34] Thus, to evaluate the diffusion of dopamine into the interior of the PEG (150 μm thick) and agar (1 mm thick) hydrogels, their color change was monitored as a function of time, Figure S2. Red-green-blue (RGB) color values at the surface and the center of the hydrogels were determined, where higher RGB values indicate darker colors corresponding to PDA formation. RGB analysis determined that PDA formation occurred rapidly (within 1 h) at the hydrogel surface. After a reaction time of 6 h, a uniform brown color was observed indicating the presence of PDA throughout the entire cross section of all hydrogels, independent of their composition. Three methods of PDA incorporation into PEG and agar hydrogels are highlighted in the Supporting Information and Figure S2; they were found to provide similar results after a reaction time of 6 h. Thus, while any of the three methods could be used, for the remainder of this study, dopamine polymerization was initiated following hydrogel formation but before swelling the hydrogels because this method was facile and provided samples with a consistent physical appearance.

Figure 1. Photographs of a PEG hydrogel before and after pMPC/PDA functionalization. Scales bars are 1 mm.

The PEG hydrogels were imaged using atomic force microscopy (AFM) in a hydrated environment after 6 h of swelling-assisted pMPC/PDA formation, Figure 2. Following pMPC/PDA formation and thorough rinsing with deionized water, the hydrogel surface was decorated with small PDA aggregates, characteristic of the mechanism of dopamine polymerization.[50,51] PDA formation in the presence of pMPC has been reported to reduce the aggregate size.[34] On the surface of the pMPC/PDA PEG hydrogels, the aggregates ranged in size from 5 to 150 nm. The aggregates were also visible on the surface of dry hydrogels that were imaged using scanning electron microscopy (SEM, not shown). SEM micrographs acquired on the cross section of PEG and agar hydrogels suggest that significantly fewer aggregates were present within the hydrogels than on their surface, Figure S3. In fact, no aggregates were observed within the agar hydrogels.

The equilibrium swelling ratios (Q) were statistically equivalent for the control and pMPC/PDA PEG hydrogels synthesized at all polymer concentrations, Table 1. This finding is interesting as PDA has previously been shown to inhibit hydrogel swelling.[12] Therefore, the strong interaction of the zwitterionic polymer with water likely overcame any swelling inhibition that would otherwise be induced by PDA. The PEG hydrogels were covalently cross-linked through methacrylate moieties; their approximate mesh size (ξ) was calculated using the Peppas modification of Flory theory.[52] The mesh size was determined to be 3.4 ± 0.2 nm, 1.9 ± 0.1 nm, and 1.0 ± 0.1 nm for 8.3, 28, and 55 wt % PEG hydrogels, respectively. In contrast, the agar hydrogels are physically cross-linked networks with large pores. Cyro-SEM has been used to approximate the pores of 1.0 wt % agar hydrogels to range from 370 to 800 nm in diameter,[53] and the equilibrium

DOI: 10.1021/acsabm.8b00001
ACS Appl. Bio Mater. 2018, 1, 33−41

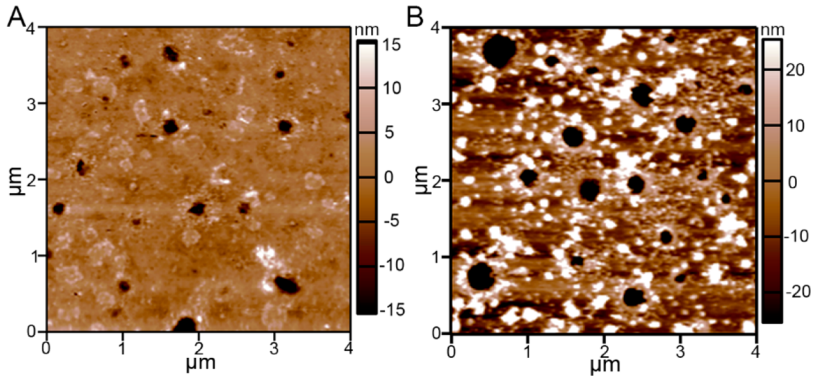

Figure 2. AFM surface topography images of hydrated (A) unmodified and (B) pMPC/PDA-modified PEG hydrogels. Representative micrographs were acquired on 55 wt % PEG hydrogels that were hydrated throughout the entire imaging process in DI water. A z-scale is provided alongside each image.

Table 1. Storage Modulus (G'), Loss Modulus (G''), Volumetric Swelling Ratio (Q), and Mesh Size (ξ) of Unmodified and pMPC/PDA-Modified PEG and Agar Hydrogels

	PEG hydrogels			pMPC/PDA PEG hydrogels			
PEG (wt %)	G' (kPa)	G'' (kPa)	Q	G' (kPa)	G'' (kPa)	Q	ξ (nm)
8.3	1.7 ± 0.1	0.02 ± 0.01	13 ± 1.6	2.0 ± 0.2	0.04 ± 0.01	11 ± 0.8	3.4 ± 0.2
28	77 ± 3	3 ± 0.3	3.8 ± 0.4	94 ± 18	3.8 ± 0.4	3.4 ± 0.1	1.9 ± 0.04
55	1300 ± 200	190 ± 5	2.2 ± 0.05	1300 ± 60	60 ± 10	2.2 ± 0.1	1.0 ± 0.1
	agar hydrogels			pMPC/PDA agar hydrogels			
agar (wt %)	G' (kPa)	G'' (kPa)		G' (kPa)	G'' (kPa)		
1.0	2.5 ± 0.4	0.06 ± 0.01		2.1 ± 0.1	0.06 ± 0.01		
3.0	30 ± 4	2.9 ± 1.3		37 ± 1.0	1.5 ± 1.8		
9.0	370 ± 50	52 ± 11		240 ± 25	60 ± 30		

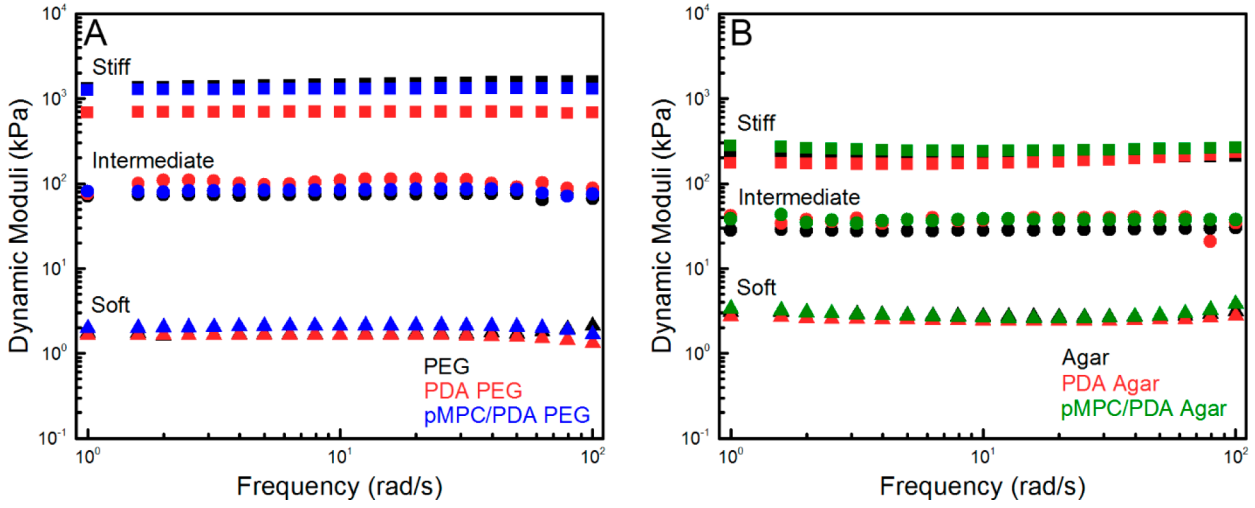

Figure 3. Representative frequency sweeps of unmodified, as well as PDA and pMPC/PDA-modified (A) PEG and (B) agar hydrogels. PEG hydrogels (8.3, 28, and 55 wt % PEG) and agar hydrogels (1.0, 3.0, and 9.0 wt % agar) are labeled as soft, intermediate, and stiff, respectively, to simplify sample labeling.

swelling of other biopolymer hydrogels has been reported to range from 400−6600% with large deviations.[54] Thus, the effect of pMPC/PDA on the equilibrium swelling of agar hydrogels could not be determined reliably. In general, the smallest pore size of agar hydrogels is much larger than that of the PEG hydrogels and therefore provided no barrier for pMPC/PDA diffusion. Thus, pMPC/PDA was successfully incorporated into both PEG and agar hydrogels despite substantial differences in their cross-linking chemistry, architecture, and network construction.

Mechanical Characteristics of pMPC/PDA-Modified PEG and Agar Hydrogels. Hydrogel stiffness is intrinsically tied to polymer concentration, with an increasing concentration leading to an increased cross-link density and stiffness.[55] Small amplitude oscillatory shear (SAOS) measurements indicated that the elastic component dominated the complex modulus and G' displayed frequency independence

DOI: 10.1021/acsabm.8b00001
ACS Appl. Bio Mater. 2018, 1, 33−41

for the PEG (8.3, 28, and 55 wt %) and agar (1.0, 3.0, and 9.0 wt %) hydrogels, Figure S4. Based on their dynamic moduli, and to simplify the naming of the hydrogels, we categorized them into three regimes: soft (1.7 ± 0.1 kPa PEG and 2.5 ± 0.4 kPa agar), intermediate (110 ± 40 kPa PEG and 30 ± 4.0 kPa agar), and stiff (1300 kPa ± 200 PEG and 370 ± 50 kPa agar).

Ideally, introducing a second polymer network, such as pMPC/PDA, would not disrupt the original hydrogel network and would either improve or maintain mechanical strength without sacrificing chemical stability.[56] Following PDA or pMPC/PDA polymerization, the mechanical properties of the PEG and agar hydrogels displayed minimal variation from the unmodified hydrogels, Figure 3 and Table 1. For example, the intermediate PEG hydrogels had statistically equivalent G' values of 110 ± 40 kPa, 100 ± 6.0 kPa, and 94 ± 18 kPa for the unmodified, PDA, and pMPC/PDA PEG hydrogels, respectively.

After PDA incorporation, the stiff PDA PEG hydrogels displayed a significant loss in mechanical strength: G' decreased from 1300 ± 230 kPa to 710 ± 20 kPa and G'' decreased from 190 ± 5.0 kPa to 20 ± 1.0 kPa. Interestingly, stiff pMPC/PDA PEG hydrogels displayed a comparable G' to the unmodified PEG hydrogels, 1300 ± 6.0 kPa, but a smaller G'' of 63 ± 13 kPa. Agar hydrogels displayed no difference in G' or G'' following PDA or pMPC/PDA polymerization for soft, intermediate, and stiff hydrogels, Figure 3B. The changes in the mechanical properties of PEG hydrogels following PDA formation are likely linked to the mesh size of the PEG network. The 1.0−3.4 nm mesh size of the PEG hydrogels generally excluded PDA aggregate diffusion into the hydrogel interior. SEM imaging of many hydrogel cross sections showed little evidence of large PDA-aggregates, Figure S2. However, the larger aggregates arising from PDA-only polymerization potentially disrupted the network structure of the stiff PEG hydrogels and contributed to a reduction in G', whereas the hydrogel network structure was unaffected by the smaller (<150 nm) pMPC/PDA aggregates. The similar mechanical properties of the agar hydrogels, before and after PDA and pMPC/PDA polymerization, are likely due to their large pore structure, reducing the effect of PDA aggregates on the mechanical properties; SEM imaging confirmed that no large aggregates were observed within the agar hydrogels.

Protein Resistance of pMPC/PDA-Modified PEG and Agar Hydrogels. The fouling resistance of PEG and agar hydrogels with and without PDA and pMPC/PDA was evaluated by a fluorescent protein assay using fibrinogen, a model serum protein. After 24 h exposure to a solution of 100 $\mu g/cm^2$ of fibrinogen, a minimal yet quantifiable amount of protein adsorption was detected via fluorescence microscopy on the PEG hydrogels, whereas a significant amount of fibrinogen adsorbed to the agar hydrogels, Figures 4, S5, and S6 and Table 2. Compared to unmodified hydrogel controls, a statistically significant improvement was observed for both PEG and agar hydrogels following PDA formation.[35] A nondetectable amount of fibrinogen adhered to the pMPC/PDA PEG hydrogels; previous literature has benchmarked this achievement as an "ultralow-fouling" behavior.[23,57] The 99% improvement in antifouling performance following pMPC/PDA incorporation indicates an impressively synergistic relationship between PEG and pMPC because PEG hydrogels are already quite resistant to protein adsorption. On the other hand, agar hydrogels are high-fouling and well-known to

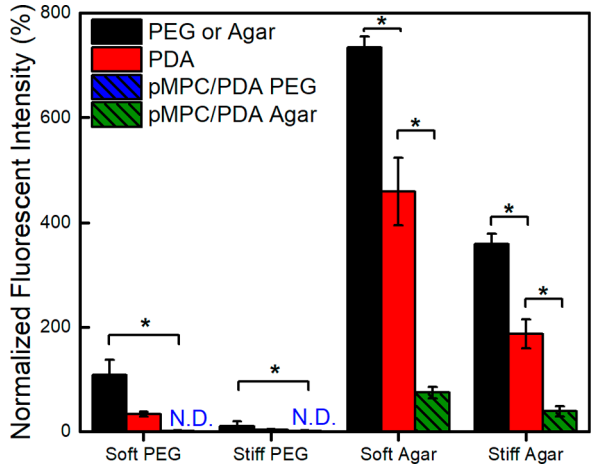

Figure 4. Protein adsorption to unmodified and pMPC/PDA-modified PEG and agar hydrogels following incubation with fibrinogen. The fluorescence intensity of irreversibly adsorbed fibrinogen was quantified and normalized against protein-free controls. Adsorption below the detection limit is labeled not detected (N.D.). One asterisk (*) denotes $p < 0.001$ significance.

Table 2. Fibrinogen Adsorption on PDA and pMPC/PDA-Modified Hydrogels Compared to Unmodified Controls

	fibrinogen adsorption (EGFP unit count)			fibrinogen adsorption (%)	
hydrogel	unmodified	+PDA	+pMPC/PDA	+PDA	+pMPC/PDA
soft PEG	110 ± 30	30 ± 4	N.D.	31	<1
stiff PEG	10 ± 10	4.0 ± 1	N.D.	36	<1
soft agar	730 ± 20	460 ± 60	70 ± 10	62	10
stiff agar	360 ± 20	190 ± 30	40 ± 10	52	11

readily adsorb protein when challenged.[58] The improvement in fibrinogen resistance on agar hydrogels was incredibly pronounced; pMPC/PDA agar hydrogels adsorbed 10 times less fibrinogen (70 ± 10 EGFP unit count) in comparison to unmodified agar hydrogels (730 ± 20 EGFP unit count). Remarkably, the inclusion of pMPC/PDA enabled the agar hydrogels to resist protein fouling almost as effectively as the PEG hydrogels.

Bacterial Resistance of pMPC/PDA-Modified PEG and Agar Hydrogels. Unmodified and pMPC/PDA-modified PEG and agar hydrogels were challenged for 24 h with two model bacterial species, Gram-positive *S. aureus* and Gram-negative *E. coli*. Glass coverslips, PDA, and pMPC/PDA thin films (on glass) served as control samples. Despite their resistance to fibrinogen adsorption, *S. aureus* and *E. coli* adhesion occurred on PEG hydrogels, Figure 5. As expected from the known prevalence of protein adsorption to agar hydrogels,[58] both bacteria adhered more readily to agar than PEG. Qualitative indications of early biofilm development, i.e., the clustering of *S. aureus* into microcolonies, were observed on the stiffest unmodified PEG and agar hydrogels, Figure S7. Consistent with our previous work,[16] bacteria coverage increased with stiffness on the unmodified hydrogels. For both bacterial species, there was a positive correlation between bacterial colony surface coverage and hydrogel stiffness on both hydrogels. For example, *E. coli* adhesion on soft PEG hydrogels (0.77%) was significantly less (p value <0.01) than on the intermediate PEG hydrogels (1.64%), and the

DOI: 10.1021/acsabm.8b00001
ACS Appl. Bio Mater. 2018, 1, 33−41

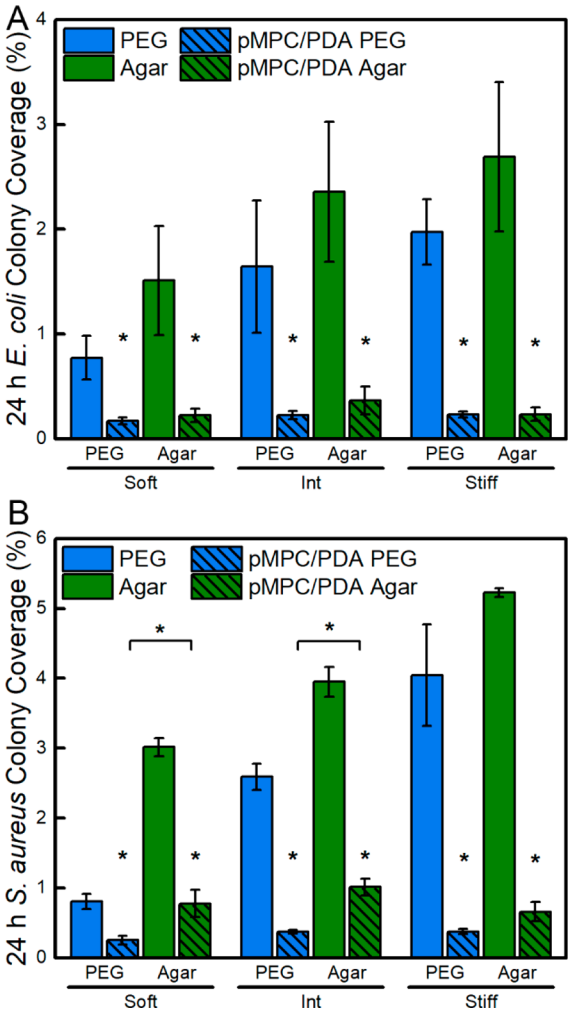

Figure 5. Adhesion of (A) *E. coli* and (B) *S. aureus* on unmodified and pMPC/PDA-modified PEG and agar hydrogels. Hydrogels are grouped by their storage moduli: soft, intermediate, and stiff. *E. coli* and *S. aureus* adhesion was statistically different (p value < 0.01) on unmodified PEG and unmodified agar hydrogels in different stiffness regimes; for simplicity, these statistical markings are not shown. The difference between unmodified and pMPC/PDA-modified hydrogels is statistically significant (p value < 0.01) for all samples and displayed on the plots. One asterisk (*) denotes p < 0.001 intrasample significance, and brackets denote p < 0.001 intersample hydrogels significance. Standard error is displayed.

intermediate PEG displayed significantly less *E. coli* adhesion than the stiff PEG hydrogels (1.97%). The same trend was displayed for *E. coli* adhesion on soft agar (1.51%), intermediate agar (2.69%), and stiff agar (3.68%), as well as *S. aureus* on each hydrogel system with increasing stiffness.

Although PDA surface modification reduced bacterial adhesion, PDA functionalization alone is insufficient to substantially resist long-term adhesion of either bacterial species, Figure S8.[59,60] For example, although PDA reduced *S. aureus* colony coverage from 6.2 ± 1.0% to 3.6 ± 1.0% compared to unmodified glass, pMPC/PDA-functionalized surfaces much more significantly reduced bacterial surface coverage, by an additional 5 times to 0.7 ± 0.1%. All of the pMPC/PDA hydrogels displayed significantly less bacterial adhesion than the unmodified controls and lacked signs of colony formation from either bacterial species. Interestingly, *E. coli* colony coverage was consistent on all surfaces following pMPC/PDA formation, including thin films (on glass) and normally high-fouling agar hydrogels. Quantitatively, *E. coli* adhesion was statistically equivalent on soft, intermediate, and stiff pMPC/PDA PEG hydrogels with colony area coverages of 0.17 ± 0.03%, 0.23 ± 0.04%, and 0.23 ± 0.03%, respectively. *E. coli* attachment was reduced by 5, 7, and 9 times on pMPC/PDA-modified PEG hydrogels compared to unmodified PEG hydrogels. Our antifouling results compare favorably to the work by Cheng et al., who found that surfaces grafted via atom transfer radical polymerization (ATRP) with a long-chain zwitterionic poly(sulfobetaine methacrylate) significantly reduced the colony coverage of *Staphylococcus epidermis* and *Pseudomonas aeruginosa* by greater than 80% compared to glass controls.[61] Further, *E. coli* colony coverages of 0.22 ± 0.07%, 0.37 ± 0.13%, and 0.23 ± 0.06% were observed on soft, intermediate, and stiff pMPC/PDA agar hydrogels; values that are statistically equivalent to pMPC/PDA thin films (on glass) (0.22 ± 0.07%) and all pMPC/PDA PEG hydrogels. The improvement in the fouling resistance of pMPC/PDA agar hydrogels is especially remarkable and demonstrates that the strong antifouling properties provided by the pMPC can be applied successfully to either hydrogel composition.

PMPC/PDA-modified PEG hydrogels exhibited superior resistance to *S. aureus* adhesion relative to pMPC/PDA-modified agar or thin films (on glass) (Figures 5B and S8). *S. aureus* adhesion was statistically equivalent on soft, intermediate, and stiff pMPC/PDA PEG hydrogels with colony area coverages of 0.25 ± 0.06%, 0.37 ± 0.02%, and 0.37 ± 0.04%, respectively. Notably, soft, intermediate, and stiff pMPC/PDA agar hydrogels displayed *S. aureus* colony area coverages of 0.78 ± 0.20%, 1.0 ± 0.12%, and 0.65 ± 0.14%, respectively. These functionalized agar hydrogels supported 4 times fewer microbes than the unmodified agar hydrogels, but significantly more microbes than the pMPC/PDA PEG hydrogels. Further, the pMPC/PDA thin films (on glass) displayed an impressive 9 times reduction in *S. aureus* adhesion, from 6.2 ± 1.0% to 0.68 ± 0.06% *S. aureus* compared to unmodified glass controls, Table S1. Therefore, the superior performance of pMPC/PDA PEG hydrogels likely resulted from a combination of the antifouling activity of both PEG and pMPC. The increased adhesion of *S. aureus* to pMPC/PDA agar compared to pMPC/PDA PEG is likely due to the unique membrane-bound protein-binding adhesins in *S. aureus* that facilitates attachment to human tissue, enhancing interaction with the bioinspired MPC structure.[62,63] This is consistent with literature reports, which demonstrate that the chemical composition and physical architecture of abiotic materials are known to induce a greater variation in *S. aureus* adhesion than *E. coli*.[64,65]

CONCLUSION

We have presented a simple and versatile technique to enhance the fouling resistance of hydrogels with polymer zwitterions, independent of the network structure and mechanical properties of the original hydrogel. Using a simple, solution-based approach, a fouling-resistant polymer zwitterion, pMPC, was integrated into PEG and agar hydrogels during hydrogel swelling to facilitate uniform pMPC/PDA incorporation without sacrificing the integrity of the original hydrogel network. The inclusion of this fouling-resistant polymer network successfully reduced fibrinogen adsorption on agar by over 90%, transforming a culture medium for bacteria into a fouling-resistant material. Relative to unmodified PEG and agar

DOI: 10.1021/acsabm.8b00001
ACS Appl. Bio Mater. 2018, 1, 33−41

hydrogels, *E. coli* and *S. aureus* adhesion was significantly reduced (up to 91%) on all hydrogels following pMPC/PDA formation. PDA-mediated integration of polymer zwitterions offers a simple and versatile platform to enhance the antifouling performance of hydrogels without altering the mechanical properties of the original hydrogel.

■ ASSOCIATED CONTENT

Supporting Information

The Supporting Information is available free of charge on the ACS Publications website at DOI: 10.1021/acsabm.8b00001.

FTIR spectra, additional methods to functionalize hydrogels, hydrogel cross sections and analysis of PDA diffusion/polymerization, cross-sectional SEM micrographs, storage and viscous moduli of hydrogels, micrographs and fluorescence spectra of fibrinogen adsorption on hydrogels, micrographs of *E. coli* and *S. aureus* adhesion, total colony area coverage of *E. coli* and *S. aureus*, and colony coverage of *E. coli* and *S. aureus* on glass (PDF)

■ AUTHOR INFORMATION

Corresponding Author

*E-mail: schiffman@ecs.umass.edu.

ORCID

Todd Emrick: 0000-0003-0460-1797

Stephen S. Nonnenmann: 0000-0002-5369-9279

Jessica D. Schiffman: 0000-0002-1265-5392

Notes

The authors declare no competing financial interest.

■ ACKNOWLEDGMENTS

The authors thank Dr. Nathan P. Birch, Natalie R. Mako, and Xiangxi Meng for assistance with experiments and helpful discussions. K.W.K. was supported by the National Research Service Award T32 GM008515 from the National Institutes of Health. This work was supported in part by a fellowship given by UMass to K.M.D. as part of the Biotechnology Training Program (NIH, National Research Service Award T32 GM108556). J.D.S. acknowledges the support of the National Science Foundation (NSF CBET-1719747).

■ REFERENCES

(1) Von Eiff, C.; Jansen, B.; Kohnen, W.; Becker, K. Infections Associated with Medical Devices: Pathogenesis, Management and Prophylaxis. *Drugs* **2005**, *65*, 179−214.

(2) Meddings, J.; Rogers, M. A. M.; Krein, S. L.; Fakih, M. G.; Olmsted, R. N.; Saint, S. Reducing Unnecessary Urinary Catheter Use and Other Strategies to Prevent Catheter-Associated Urinary Tract Infection: An Integrative Review. *BMJ. Qual Saf* **2014**, *23*, 277−289.

(3) O'Grady, N. P.; Alexander, M.; Burns, L. A.; Dellinger, E. P.; Garland, J.; Heard, S. O.; Lipsett, P. A.; Masur, H.; Mermel, L. A.; Pearson, M. L.; Raad, I. I.; Randolph, A.; Rupp, M. E.; Saint, S. Guidelines for the Prevention of Intravascular Catheter-Related Infections. *Clin. Infect. Dis.* **2011**, *52*, 1087−1099.

(4) Klevens, R. M.; Edwards, J. R.; Richards, C. L.; Horan, T. C.; Gaynes, R. P.; Pollock, D. A.; Cardo, D. M. Estimating Health Care-Associated Infections and Deaths in U.S. Hospitals, 2002. *Public Health Rep.* **2007**, *122*, 160−166.

(5) Kennedy, E. H.; Greene, M. T.; Saint, S. Estimating Hospital Costs of Catheter-Associated Urinary Tract Infection. *J. Hosp. Med.* **2013**, *8*, 519−522.

(6) Magill, S. S.; Edwards, J. R.; Bamberg, W.; Beldavs, Z. G.; Dumyati, G.; Kainer, M. A.; Lynfield, R.; Maloney, M.; McAllister-Hollod, L.; Nadle, J.; Ray, S. M.; Thompson, D. L.; Wilson, L. E.; Fridkin, S. K. Multistate Point-Prevalence Survey of Health Care−Associated Infections. *N. Engl. J. Med.* **2014**, *370*, 1198−1208.

(7) Lawrence, E. L.; Turner, I. G. Materials for Urinary Catheters: A Review of Their History and Development in the UK. *Med. Eng. Phys.* **2005**, *27*, 443−453.

(8) Jagur-Grodzinski, J. Nanostructured Polyolefins/Clay Composites: Role of the Molecular Interaction at the Interface. *Polym. Adv. Technol.* **2006**, *17*, 395−418.

(9) Beiko, D. T.; Knudsen, B. E.; Watterson, J. D.; Cadieux, P. A.; Reid, G.; Denstedt, J. D. Urinary Tract Biomaterials. *J. Urol.* **2004**, *171*, 2438−2444.

(10) Banerjee, I.; Pangule, R. C.; Kane, R. S. Antifouling Coatings: Recent Developments in the Design of Surfaces That Prevent Fouling by Proteins, Bacteria, and Marine Organisms. *Adv. Mater.* **2011**, *23*, 690−718.

(11) Krishnan, S.; Weinman, C. J.; Ober, C. K. Advances in Polymers for Anti-Biofouling Surfaces. *J. Mater. Chem.* **2008**, *18*, 3405−3413.

(12) Herrwerth, S.; Eck, W.; Reinhardt, S.; Grunze, M. Factors That Determine the Protein Resistance of Oligoether Self-Assembled Monolayers - Internal Hydrophilicity, Terminal Hydrophilicity, and Lateral Packing Density. *J. Am. Chem. Soc.* **2003**, *125*, 9359−9366.

(13) Guégan, C.; Garderes, J.; Le Pennec, G.; Gaillard, F.; Fay, F.; Linossier, I.; Herry, J. M.; Fontaine, M. N. B.; Réhel, K. V. Alteration of Bacterial Adhesion Induced by the Substrate Stiffness. *Colloids Surf., B* **2014**, *114*, 193−200.

(14) Gallardo, A.; Martínez-Campos, E.; García, C.; Cortajarena, A. L.; Rodríguez-Hernández, J. Hydrogels with Modulated Ionic Load for Mammalian Cell Harvesting with Reduced Bacterial Adhesion. *Biomacromolecules* **2017**, *18*, 1521−1531.

(15) Kolewe, K. W.; Zhu, J.; Mako, N. R.; Nonnenmann, S. S.; Schiffman, J. D. Bacterial Adhesion Is Affected by the Thickness and Stiffness of Poly(Ethylene Glycol) Hydrogels. *ACS Appl. Mater. Interfaces* **2018**, *10*, 2275−2281.

(16) Kolewe, K.; Peyton, S. R.; Schiffman, J. D. Fewer Bacteria Adhere to Softer Hydrogels. *ACS Appl. Mater. Interfaces* **2015**, *7*, 19562−19569.

(17) Ventola, C. L. The Antibiotic Resistance Crisis: Part 1: Causes and Threats. *P T A peer-reviewed J. Formul. Manag.* **2015**, *40*, 277−283.

(18) Arias, C. A.; Murray, B. E. Antibiotic-Resistant Bugs in the 21st Century — A Clinical Super-Challenge. *N. Engl. J. Med.* **2009**, *360*, 439−443.

(19) Chen, S.; Li, L.; Zhao, C.; Zheng, J. Surface Hydration: Principles and Applications toward Low-Fouling/Nonfouling Biomaterials. *Polymer* **2010**, *51*, 5283−5293.

(20) Cao, B.; Tang, Q.; Cheng, G. Recent Advances of Zwitterionic Carboxybetaine Materials and Their Derivatives. *J. Biomater. Sci., Polym. Ed.* **2014**, *25*, 1502−1513.

(21) Tegoulia, V. a.; Rao, W.; Kalambur, A. T.; Rabolt, J. F.; Cooper, S. L. Surface Properties, Fibrinogen Adsorption, and Cellular Interactions of a Novel Phosphorylcholine-Containing Self-Assembled Monolayer on Gold. *Langmuir* **2001**, *17*, 4396−4404.

(22) Kuang, J.; Messersmith, P. B. Universal Surface-Initiated Polymerization of Antifouling Zwitterionic Brushes Using a Mussel-Mimetic Peptide Initiator. *Langmuir* **2012**, *28*, 7258−7266.

(23) Jiang, S.; Cao, Z. Ultralow-Fouling, Functionalizable, and Hydrolyzable Zwitterionic Materials and Their Derivatives for Biological Applications. *Adv. Mater.* **2010**, *22*, 920−932.

(24) Zhang, Z.; Chao, T.; Liu, L. Y.; Cheng, G.; Ratner, B. D.; Jiang, S. Zwitterionic Hydrogels: An in Vivo Implantation Study. *J. Biomater. Sci., Polym. Ed.* **2009**, *20*, 1845−1859.

(25) Zhang, L.; Cao, Z.; Bai, T.; Carr, L.; Ella-Menye, J.-R.; Irvin, C.; Ratner, B. D.; Jiang, S. Zwitterionic Hydrogels Implanted in Mice Resist the Foreign-Body Reaction. *Nat. Biotechnol.* **2013**, *31*, 553−556.

(26) Cao, B.; Li, L.; Tang, Q.; Cheng, G. The Impact of Structure on Elasticity, Switchability, Stability and Functionality of an All-in-One Carboxybetaine Elastomer. *Biomaterials* **2013**, *34*, 7592−7600.
(27) Ning, J.; Li, G.; Haraguchi, K. Synthesis of Highly Stretchable, Mechanically Tough, Zwitterionic Sulfobetaine Nanocomposite Gels with Controlled Thermosensitivities. *Macromolecules* **2013**, *46*, 5317−5328.
(28) Yin, H.; Akasaki, T.; Lin Sun, T.; Nakajima, T.; Kurokawa, T.; Nonoyama, T.; Taira, T.; Saruwatari, Y.; Ping Gong, J. Double Network Hydrogels from Polyzwitterions: High Mechanical Strength and Excellent Anti-Biofouling Properties. *J. Mater. Chem. B* **2013**, *1*, 3685−3693.
(29) Carr, L. R.; Zhou, Y.; Krause, J. E.; Xue, H.; Jiang, S. Uniform Zwitterionic Polymer Hydrogels with a Nonfouling and Functionalizable Crosslinker Using Photopolymerization. *Biomaterials* **2011**, *32*, 6893−6899.
(30) Cao, B.; Tang, Q.; Li, L.; Humble, J.; Wu, H.; Liu, L.; Cheng, G. Switchable Antimicrobial and Antifouling Hydrogels with Enhanced Mechanical Properties. *Adv. Healthcare Mater.* **2013**, *2*, 1096−1102.
(31) Lee, H.; Dellatore, S. M.; Miller, W. M.; Messersmith, P. B. Mussel-Inspired Surface Chemistry for Multifunctional Coatings. *Science* **2007**, *318*, 426−430.
(32) Liu, Y.; Ai, K.; Lu, L. Polydopamine and Its Derivative Materials: Synthesis and Promising Applications in Energy, Environmental, and Biomedical Fields. *Chem. Rev.* **2014**, *114*, 5057−5115.
(33) Zhou, R.; Ren, P. F.; Yang, H. C.; Xu, Z. K. Fabrication of Antifouling Membrane Surface by Poly(Sulfobetaine Methacrylate)/Polydopamine Co-Deposition. *J. Membr. Sci.* **2014**, *466*, 18−25.
(34) Chang, C.-C.; Kolewe, K. W.; Li, Y.; Kosif, I.; Freeman, B. D.; Carter, K. R.; Schiffman, J. D.; Emrick, T. Underwater Superoleophobic Surfaces Prepared from Polymer Zwitterion/Dopamine Composite Coatings. *Adv. Mater. Interfaces* **2016**, *3*, 521−530.
(35) Kolewe, K. W.; Dobosz, K. M.; Rieger, K. A.; Chang, C.-C.; Emrick, T.; Schiffman, J. D. Antifouling Electrospun Nanofiber Mats Functionalized with Polymer Zwitterions. *ACS Appl. Mater. Interfaces* **2016**, *8*, 27585−27593.
(36) Sundaram, H. S.; Han, X.; Nowinski, A. K.; Brault, N. D.; Li, Y.; Ella-Menye, J. R.; Amoaka, K. A.; Cook, K. E.; Marek, P.; Senecal, K.; Jiang, S. Achieving One-Step Surface Coating of Highly Hydrophilic Poly(Carboxybetaine Methacrylate) Polymers on Hydrophobic and Hydrophilic Surfaces. *Adv. Mater. Interfaces* **2014**, *1*, 1−8.
(37) Kang, S. M.; Hwang, N. S.; Yeom, J.; Park, S. Y.; Messersmith, P. B.; Choi, I. S.; Langer, R.; Anderson, D. G.; Lee, H. One-Step Multipurpose Surface Functionalization by Adhesive Catecholamine. *Adv. Funct. Mater.* **2012**, *22*, 2949−2955.
(38) Zhang, C.; Li, H.-N.; Du, Y.; Ma, M.-Q.; Xu, Z.-K. $CuSO_4$/H_2O_2-Triggered Polydopamine/Poly(Sulfobetaine Methacrylate) Coatings for Antifouling Membrane Surfaces. *Langmuir* **2017**, *33*, 1210−1216.
(39) Cencer, M.; Liu, Y.; Winter, A.; Murley, M.; Meng, H.; Lee, B. P. Effect of PH on the Rate of Curing and Bioadhesive Properties of Dopamine Functionalized Poly(Ethylene Glycol) Hydrogels. *Biomacromolecules* **2014**, *15*, 2861−2869.
(40) Liu, Y.; Meng, H.; Konst, S.; Sarmiento, R.; Rajachar, R.; Lee, B. P. Injectable Dopamine-Modified Poly(Ethylene Glycol) Nanocomposite Hydrogel with Enhanced Adhesive Property and Bioactivity. *ACS Appl. Mater. Interfaces* **2014**, *6*, 16982−16992.
(41) Sun, P.; Wang, J.; Yao, X.; Peng, Y.; Tu, X.; Du, P.; Zheng, Z.; Wang, X. Facile Preparation of Mussel-Inspired Polyurethane Hydrogel and Its Rapid Curing Behavior. *ACS Appl. Mater. Interfaces* **2014**, *6*, 12495−12504.
(42) Liu, V. A.; Bhatia, S. N. Three-Dimensional Patterning of Hydrogels Containing Living Cells. *Biomed. Microdevices* **2002**, *4*, 257−266.
(43) Bhuchar, N.; Deng, Z.; Ishihara, K.; Narain, R. Detailed Study of the Reversible Addition−fragmentation Chain Transfer Polymerization and Co-Polymerization of 2-Methacryloyloxyethyl Phosphorylcholine. *Polym. Chem.* **2011**, *2*, 632−639.
(44) Wertz, C. F.; Santore, M. M. Adsorption and Relaxation Kinetics of Albumin and Fibrinogen on Hydrophobic Surfaces: Single-Species and Competitive Behavior. *Langmuir* **1999**, *15*, 8884−8894.
(45) Robeson, J. L.; Tilton, R. D. Effect of Concentration Quenching on Fluorescence Recovery after Photobleaching Measurements. *Biophys. J.* **1995**, *68*, 2145−2155.
(46) Pang, Y. Y.; Schwartz, J.; Thoendel, M.; Ackermann, L. W.; Horswill, A. R.; Nauseef, W. M. Agr-Dependent Interactions of *Staphylococcus aureus* USA300 with Human Polymorphonuclear Neutrophils. *J. Innate Immun.* **2010**, *2*, 546−559.
(47) Zodrow, K. R.; Schiffman, J. D.; Elimelech, M. Biodegradable Polymer (PLGA) Coatings Featuring Cinnamaldehyde and Carvacrol Mitigate Biofilm Formation. *Langmuir* **2012**, *28*, 13993−13999.
(48) Fux, C.; Wilson, S.; Stoodley, P. Detachment Characteristics and Oxacillin Resistance of *Staphoccocus aureus* Biofilm Emboli in an In Vitro Catheter Infection Model. *J. Bacteriol.* **2004**, *186*, 4486−4491.
(49) Chung, K. K.; Schumacher, J. F.; Sampson, E. M.; Burne, R. A.; Antonelli, P. J.; Brennan, A. B. Impact of Engineered Surface Microtopography on Biofilm Formation of *Staphylococcus aureus*. *Biointerphases* **2007**, *2*, 89−94.
(50) Hong, S.; Na, Y. S.; Choi, S.; Song, I. T.; Kim, W. Y.; Lee, H. Non-Covalent Self-Assembly and Covalent Polymerization Co-Contribute to Polydopamine Formation. *Adv. Funct. Mater.* **2012**, *22*, 4711−4717.
(51) Ding, Y.; Weng, L.-T.; Yang, M.; Yang, Z.; Lu, X.; Huang, N.; Leng, Y. Insights into the Aggregation/Deposition and Structure of a Polydopamine Film. *Langmuir* **2014**, *30*, 12258−12269.
(52) Canal, T.; Peppas, N. A. Correlation between Mesh Size and Equilibrium. *J. Biomed. Mater. Res.* **1989**, *23*, 1183−1193.
(53) Rahbani, J.; Behzad, A. R.; Khashab, N. M.; Al-Ghoul, M. Characterization of Internal Structure of Hydrated Agar and Gelatin Matrices by Cryo-SEM. *Electrophoresis* **2013**, *34*, 405−408.
(54) Birch, N. P.; Barney, L. E.; Pandres, E.; Peyton, S. R.; Schiffman, J. D. Thermal-Responsive Behavior of a Cell Compatible Chitosan/Pectin Hydrogel. *Biomacromolecules* **2015**, *16*, 1837−1843.
(55) Seliktar, D. Designing Cell-Compatible Hydrogels. *Science* **2012**, *336*, 13−17.
(56) Haque, M. A.; Kurokawa, T.; Gong, J. P. Super Tough Double Network Hydrogels and Their Application as Biomaterials. *Polymer* **2012**, *53*, 1805−1822.
(57) Tsai, W. B.; Grunkemeier, J. M.; Horbett, T. A. Human Plasma Fibrinogen Adsorption and Platelet Adhesion to Polystyrene. *J. Biomed. Mater. Res.* **1999**, *44*, 130−139.
(58) Chen, H.; Chen, Q.; Hu, R.; Wang, H.; Newby, B. Z.; Chang, Y.; Zheng, J. Mechanically Strong Hybrid Double Network Hydrogels with Antifouling Properties. *J. Mater. Chem. B* **2015**, *3*, 5426−5435.
(59) Sileika, T. S.; Kim, H.; Maniak, P.; Messersmith, P. B. Antibacterial Performance of Polydopamine-Modified Polymer Surfaces Containing Passive and Active Components. *ACS Appl. Mater. Interfaces* **2011**, *3*, 4602−4610.
(60) Cui, J.; Ju, Y.; Liang, K.; Ejima, H.; Lörcher, S.; Gause, K. T.; Richardson, J. J.; Caruso, F. Nanoscale Engineering of Low-Fouling Surfaces through Polydopamine Immobilisation of Zwitterionic Peptides. *Soft Matter* **2014**, *10*, 2656−2663.
(61) Cheng, G.; Zhang, Z.; Chen, S.; Bryers, J. D.; Jiang, S. Inhibition of Bacterial Adhesion and Biofilm Formation on Zwitterionic Surfaces. *Biomaterials* **2007**, *28*, 4192−4199.
(62) Götz, F. *Staphylococcus* and Biofilms. *Mol. Microbiol.* **2002**, *43*, 1367−1378.
(63) Beloin, C.; Houry, A.; Froment, M.; Ghigo, J. M.; Henry, N. A Short-Time Scale Colloidal System Reveals Early Bacterial Adhesion Dynamics. *PLoS Biol.* **2008**, *6*, 1549−1558.
(64) Gungor, B.; Esen, Ş.; Gök, A.; Yilmaz, H.; Malazgirt, Z.; Leblebicioğlu, H. Comparison of the Adherence of *E. Coli* and *S. Aureus* to Ten Different Prosthetic Mesh Grafts: In Vitro Experimental Study. *Indian J. Surg.* **2010**, *72*, 226−231.

DOI: 10.1021/acsabm.8b00001
ACS Appl. Bio Mater. 2018, 1, 33−41

(65) Hsieh, Y. -L; Merry, J. The Adherence of *Staphylococcus aureus*, *Staphylococcus epidermidis* and *Escherichia coli* on Cotton, Polyester and Their Blends. *J. Appl. Bacteriol.* **1986**, *60*, 535−544.

DOI: 10.1021/acsabm.8b00001
ACS Appl. Bio Mater. 2018, 1, 33−41